

SEASONAL PERFORMANCE ASSESSMENT OF VARIOUS PV TECHNOLOGIES IN A DESERT CLIMATE THROUGH DEVICE SIMULATIONS AND OUTDOOR MEASUREMENTS

Th. Katsaounis^{1,3,4,*}, K. Kotsovos², I. Gereige², A. Basaheeh², M. Abdullah², A. Khayat², E. Al Habshi², A. Al-Saggaf² and A. Tzavaras¹

¹Computer Electrical and Mathematical Science & Engineering (CEMSE), King Abdullah University of Science and Technology (KAUST), Thuwal, Saudi Arabia

²Saudi Aramco R&D Center, Carbon Management Division, Dhahran, Saudi Arabia

³Institute of Applied and Computational Mathematics (IACM), Foundation for Research and Technology - Hellas (FORTH), Heraklion, Greece

⁴Dept. of Math. & Applied Mathematics, Univ. of Crete, Heraklion, Greece

*Corresponding author: Computer Electrical and Mathematical Science & Engineering (CEMSE), KAUST, Thuwal, Saudi Arabia, email: theodoros.katsaounis@kaust.edu.sa

ABSTRACT: Middle East is considered as one of the most promising areas for PV deployment due to its vast solar potential. Successful deployment of PV systems in the region is challenging, however, due to local weather conditions. Frequent dust storms in these areas cause heavy soiling on PV module surface and significantly affect the solar panels performance. In addition, the combination of high ambient temperatures and increased UV irradiance levels pose additional challenges in PV module reliability. This work focuses on the influence of local climate effects on the performance and energy yield of various PV module technologies by processing local weather data over various periods. Simulation data are validated with outdoor IV measurements on various types of commercial c-Si based PV modules, located at KAUST University, Western Region of Saudi Arabia.

Keywords: c-Si, Silicon Solar Cell, PERC, Bifacial, Modelling, Simulation, Performance

1 INTRODUCTION

Recent advances in solar cell research and material improvements in novel PV structures such as perovskites enable significantly increased efficiencies especially when combined with c-Si devices in tandem. Such tandem cells have reached conversion efficiencies in excess of 29% [1], while process advances in c-Si heterojunction (HJT) technology using back contact structure have also reached record performance of 26.7% [2]. These improvements can potentially minimize the levelized cost of electricity (LCOE) in PV systems, especially at countries with high solar potential such as Saudi Arabia in the Middle East Region, where the average annual Global Horizontal Irradiance (GHI) is 2200 kWh/m² [3]. These conditions allow for a very competitive energy production cost as demonstrated by the recent record-breaking bid for the Sakaka 300 MW PV project, at a tariff of 2.34 US-cents per kWh [4]. Despite this fact, successful deployment of PV systems in the region is challenging due to local weather conditions.

Dust storms are very frequent in these areas, which

not only cause heavy soiling on PV module surface but may also significantly affect the form and intensity of the solar spectrum due to airborne dust particles which scatter sunlight. In addition, the combination of high ambient temperatures and increased irradiance levels pose additional challenges in PV module performance and reliability.

This work focuses on the influence of local climate effects on the performance and energy yield of various PV module technologies by processing local weather data over various periods. Simulation data are validated with outdoor IV measurements on various types of commercial c-Si based PV modules, located at KAUST University, Western Region of Saudi Arabia.

In addition, this study also focuses on the effects of spectral changes and the influence of airborne dust particles to the solar radiation incident at the PV module surface. Seasonal performance variations of various solar cell technologies using local spectral data are also investigated.

2 DEVICE SIMULATOR MODEL

The system of carrier transport equations is solved numerically using the finite element method. An implicit-explicit variant of Newton's method is used to linearize the system and solve each equation separately thus reducing the computational cost considerably. The computational domain was covered by a triangulation, while mesh adaptivity, is used to resolve the Dirac-like behavior of the incident light on the cell surface as well as to capture the steep gradients of the solution around the back contact. The solver was tested and compared with various well-known open source solar cell device simulators. The solar cell device simulator also includes additional features to take into account metal grid shading, reflection and temperature effects. The model was extended to simulate heterojunction (HJT) devices with structure as shown on figure 1 (bottom) by modifying the boundary conditions to incorporate the a-Si passivating layers on both surfaces. Parasitic absorption of the a-Si and thin conducting (TCO) layers was also taken into account. Further details regarding the mathematical model concept and its underlying mathematical formulation can be found in [3].

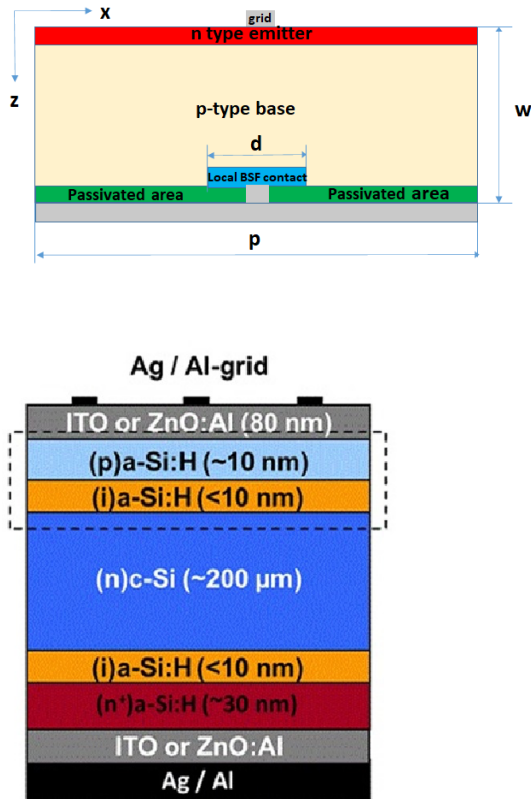


Figure 1. Geometry model of a monofacial PERC (top), and a typical HJT structure configuration (bottom).

Part of the code was developed using the FreeFem++ finite element computational framework [4]. The computational time to obtain an IV-curve consisting on

the average of 120 points varied from 10 – 30 min. It's remarked that the customized solver (KASCS) uses an adaptive algorithm to choose the voltage step during the calculation of an IV-curve. An example of IV curves for PERC & HJT solar cells simulated on a typical summer day around noon for the selected outdoor location at KAUST is shown on figure 2.

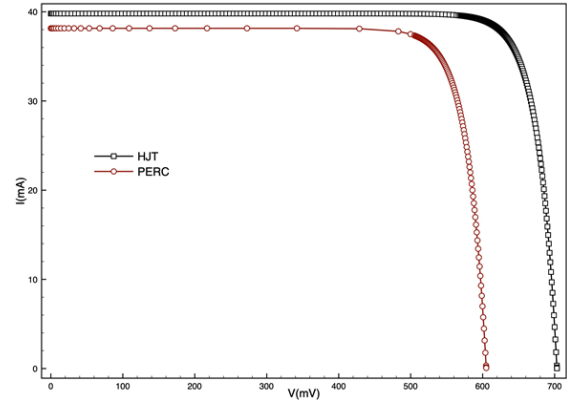


Figure 2. Typical simulated PERC and HJT IV-curves simulated on a typical summer day around noon for the selected outdoor location at KAUST.

The numerous simulations were performed on the **CRAY XC40** (Shaheen) of the Supercomputing Laboratory at King Abdullah University of Science & Technology (KAUST) in Thuwal, Saudi Arabia.

3 EXPERIMENTAL SETUP

The outdoor experimental system is installed at KAUST in Thuwal, Western region of Saudi Arabia at the New Energy Oasis (NEO) test field near the Red Sea coast (22.30 N, 39.10 E). The system consists of the following components:

- A set of commercial PV modules, including polycrystalline Si and monocrystalline HJT, with ground mounting system
- IV measuring system with radiation sensors, industrial PC and datalogger
- Solar resource measurement station with pyranometers, spectroradiometer and sky camera

The modules selected for the energy yield measurements of this study consist of a polycrystalline Al-BSF Si PV module, a PERC and a HJT, where their electrical characteristics based on their manufacturer datasheet are shown on Table 1. The modules were installed in a standard Al profile mounting system with South facing orientation, at 25 degree tilt angle. Each of them was connected to an IV tracer measuring system with multiple inputs [5] in order to monitor the electrical characteristics of each one separately.

The solar resource measurement station is installed in the same outdoor field, near the site where the PV module

measurement setup is located. The setup as includes four sensors to perform precise measurements of the three solar radiation components: Global Horizontal Irradiance (GHI), Direct Normal Irradiance (DNI), Diffuse Horizontal Irradiance (DHI) and the global spectral distribution (s-GHI). It also includes a sky camera to take hemispheric pictures of the sky. The system was designed and installed by TUV Rheinland [5].

| PV structure | Al-BSF | HJT | PERC |
|----------------|----------|---------|----------|
| Technology | Poly -Si | Mono Si | Poly -Si |
| Cell number | 60 | 60 | 72 |
| P_{max} (W) | 255 | 320 | 340 |
| I_{sc} (A) | 9 | 9.24 | 9.59 |
| V_{oc} (V) | 37.4 | 43.8 | 47.07 |
| FF (%) | 75.75 | 79.06 | 75.32 |
| Efficiency (%) | 15.85 | 19.5 | 17.1 |

Table 1. PV module specifications based on manufacturer’s datasheets.

4 RESULTS

4.1 Seasonal spectral variations impact on PV performance

Photovoltaic system performance is affected by variations in the input sunlight spectrum caused by different factors such as seasonal changes, sun’s position in the sky, etc. In addition various PV technologies show different spectral responses depending on the bandgap of the material as well as the solar cell structure, which affects their conversion efficiency.

A useful indicator to quantify the effects of spectrum variations in PV performance is the spectral factor (SF). The spectral factor – or mismatch factor – is a parameter aimed at evaluating the difference of the PV performance between an actual solar spectrum and the standard AM 1.5G. This is defined by the following formula [6] for single junction devices:

$$SF = \frac{\int E_B(\lambda)SR(\lambda)d\lambda}{\int E_B^R(\lambda)SR(\lambda)d\lambda} * \frac{\int E_B^R(\lambda)d\lambda}{\int E_B(\lambda)d\lambda} \quad (1)$$

$E_B^R(\lambda)$ & $E_B(\lambda)$ represent the reference global & the actual spectrum ($W m^{-2} nm^{-1}$) respectively, while $SR(\lambda)$ the spectral response of the device (A/W) at STC temperature conditions. In the case of tandem structures,

where j is an index identifying each junction of the cell, the spectral factor can be defined below:

$$SF_{tandem} = \frac{\min_j\{\int E_B(\lambda)SR_j(\lambda)d\lambda\}}{\min_j\{\int E_B^R(\lambda)SR_j(\lambda)d\lambda\}} * \frac{\int E_B^R(\lambda)d\lambda}{\int E_B(\lambda)d\lambda} \quad (2)$$

The calculations are performed using spectral data collected over a three-year period using the experimental setup described in the previous section and spectral response measurements for various PV technologies based on c-Si (Al-BSF, PERC, HJT), a perovskite tandem structure [7] and organic PV (OPV) devices (single & tandem [8-9]). The calculation results for two representative months of 2017 (December & June) are illustrated on Figure 3.

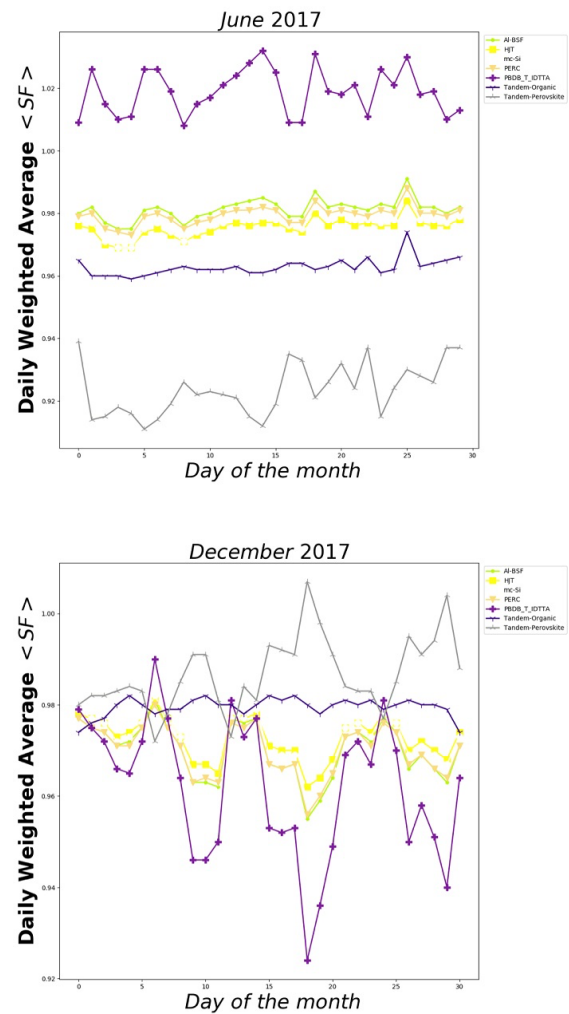


Figure 3. Daily weighted average Spectral Factor (SF) for various c-Si PV technologies (Al-BSF, PERC, HJT), organic PV (OPV) single & tandem structure and a perovskite- Si multijunction device for the months June & December 2017.

Both graphs of Figure 3 demonstrate that the performance of all devices has some considerable fluctuations depending on the day as well as the season. In general, during the winter month of December, the spectral factor is lower than unity for all technologies investigated, while during the summer month of June is

higher for the OPV and perovskite cells. It's worth noting that all Si based technologies perform very close to each other and are slightly affected by seasonal changes, since they are based on the same material, and their bandgap is narrower compared to OPV & perovskites. The tandem structures are also more sensitive to spectrum changes as these affects top & bottom cell matching, where during the winter month of December their spectral factor is higher compared to the summer one of June. Therefore, tuning the thickness and absorber properties of each junction is required to optimize energy yield in tandem structures.

4.2 Energy Yield comparison results

In this section we compare the electrical performance characteristics of the PV modules obtained from the simulations with the corresponding measured ones. Figure 4 shows a typical example of the measured energy yield (EY) for a set of poly Si, PERC & HJT modules measured during the period 10-21 October 2019 at KAUST for 25° tilt angle installation. The chart shows that the high efficiency modules (PERC & HJT) slightly outperform the standard poly Si one, while the HJT delivers the highest energy yield during this period, which can be attributed to its lower temperature coefficient.

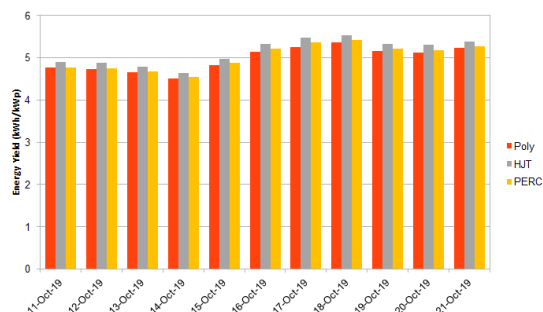


Figure 4 Measured daily energy yield for different PV module technologies for the period 10-21 October 2019.

Figure 5 illustrates the daily yield output for the HJT module during the period 2-29 June 2019. The graph shows good agreement between the experimental curve (red line) and the simulated one (blue color) with the latter following exactly the measured daily energy yield changes, thus validating our model. The offset between the simulated and experimental curve is due to external series & shunt resistance of the measured module. To correct this offset a statistical machine learning algorithm is applied using an initial set of measurements as training data to calculate the external series and shunt resistance. The third curve (black color) is obtained after the correction, where the agreement of corrected daily yield output with the experimental data is remarkable, thus validating the aforementioned process.

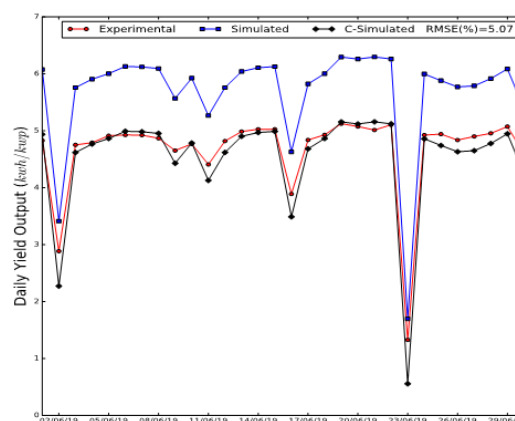


Figure 5. Daily yield output (kWh/kwp) for a HJT PV module installed in KAUST at 25° tilt angle. Measurement period displayed was 02/06/2019 - 29/06/2019.

In summary, the above analysis demonstrates that the customized simulation model can accurately predict the output performance of various solar cell structures, therefore it can be used as a guide to select the optimum PV technology for the local climate.

5 CONCLUSIONS

In this study an extended analysis was presented to investigate the influence of local climate effects on the performance and energy yield of various PV module technologies by processing local weather data collected over various periods nearby the western coast of Saudi Arabia. The results of a customized solar cell device simulator developed to take into account spectral and temperature effects were also presented and validated with experimental measurements, where very good agreement was observed between simulated and experimental results.

Our results further suggest that the simulation model can accurately predict the output performance of various solar cell structures, which can be utilized to select the optimum PV technology for the local conditions.

ACKNOWLEDGEMENTS

The authors acknowledge the support of the Supercomputing Laboratory at King Abdullah University of Science & Technology (KAUST) in Thuwal, Saudi Arabia; the KAUST Economic development for their technical support and Saudi Aramco R&D Center - Carbon Management Division for their financial support through grant RGC#3893.

REFERENCES

- [1] S. Alawaji, *Renewable & Sustainable Energy Reviews* 5 (2001) 59.
- [2] ACWA Power wins 300MW Saudi solar project, <https://www.pv-tech.org/news/acwa-power-wins-saudi-300mw-solar-project>
- [3] Th. Katsaounis, K. Kotsovos, I. Gereige, A. Al-Saggaf, and A. Tzavaras, *Solar Energy*, 158 (2017) 34.
- [4] F. Hecht, *J. Numer. Math.*, 20 (2012) 251.
- [5] Th.Katsaounis, K.Kotsovos, I. Gereige, A.Basaheeh, M.Abdullah, A.Khayat, E. Al-Habshi, A.Al-Saggaf, and A.E.Tzavaras, *Renewable Energy*, 143 (2019) 1285.
- [6] P. Rodrigo, E. F. Fernández, F. Almonacid, P. J. Pérez- Higuera, *Solar Energy Materials & Solar Cells*, 163 (2017) 73.
- [7] E. Aydin, M. De Bastiani, X. Yang, M. Sajjad, F. Aljamaan, Y. Smirnov, M.N. Hedhili, W. Liu, T.G. Allen, L. Xu, E. Van Kerschaver, M. Morales-Masis, Udo Schwingenschlögl and S. De Wolf. *Advanced Functional Materials* (2019) 1901741.
- [8] Y. Firdaus, Q. He, Y. Lin, F. Anggoro, V. Corre, E. Yengel, A. Balawi, A. Seikhan, F. Laquai, C. Langhammer, F. Liu, M. Heeney and T. D. Anthopoulos, *Journal of Materials Chemistry A*, (2020), 8, 1164.
- [9] L. Meng, Y. Zhang, X. Wan, C Li, X. Zhang, Y. Wang, X. Ke, Z. Xiao, L. Ding, R. Xia, H. Yip, Y. Cao and Y. Chen, *Science*, 361 (2018), 1094.